Distribution history and climatic controls of the Late Miocene Pikermian chronofauna

Jussi T. Eronen[a,1], Majid Mirzaie Ataabadi[a], Arne Micheels[b], Aleksis Karme[a], Raymond L. Bernor[c,d], and Mikael Fortelius[a,e]

[a]Department of Geology and [e]Institute of Biotechnology, FIN-00014 University of Helsinki, Finland; [b]Senckenberg Forschungsinstitut und Naturmuseum, Biodiversität und Klima Forschungszentrum (BiK-F), Senckenberganlage 25, D-60325, Frankfurt am Main, Germany; [c]Sedimentary Geology and Paleobiology Program, Geosciences/Earth Sciences, National Science Foundation, 4201 Wilson Boulevard, Arlington, VA 22230; and [d]College of Medicine, Department of Anatomy, Laboratory of Evolutionary Biology, Howard University, 520 W Street Northwest, Washington, D.C. 20059

Edited by David Pilbeam, Harvard University, Cambridge, MA, and approved May 12, 2009 (received for review March 9, 2009)

The Late Miocene development of faunas and environments in western Eurasia is well known, but the climatic and environmental processes that controlled its details are incompletely understood. Here we map the rise and fall of the classic Pikermian fossil mammal chronofauna between 12 and 4.2 Ma, using genus-level faunal similarity between localities. To directly relate land mammal community evolution to environmental change, we use the hypsodonty paleoprecipitation proxy and paleoclimate modeling. The geographic distribution of faunal similarity and paleoprecipitation in successive timeslices shows the development of the open biome that favored the evolution and spread of the open-habitat adapted large mammal lineages. In the climate model run, this corresponds to a decrease in precipitation over its core area south of the Paratethys Sea. The process began in the latest Middle Miocene and climaxed in the medial Late Miocene, about 7–8 million years ago. The geographic range of the Pikermian chronofauna contracted in the latest Miocene, a time of increasing summer drought and regional differentiation of habitats in Eastern Europe and Southwestern Asia. Its demise at the Miocene-Pliocene boundary coincides with an environmental reversal toward increased humidity and forestation, changes inevitably detrimental to open-adapted, wide-ranging large mammals.

fossil mammals | paleoclimate | Pikermi | similarity index

The Late Miocene spread of increasingly open and seasonal environments and their associated biota in the continental realm of Western Eurasia is well known (1–5), The changes in the fossil mammal communities was first analyzed on a continental scale by Bernor et al. (1), who recognized an overall change in community structure toward more open country-adapted faunas. These Late Miocene fossil mammal communities with open-country taxa are usually referred to as Pikermian faunas, after Pikermi near Athens, Greece, one of the first and richest localities discovered. Bernor et al. (6) characterized the Pikermian paleobiome as seasonal sclerophyllous evergreen woodland, and Solounias et al. (7) suggested that there was approximately 1,000 mm annual precipitation with strong seasonality. The Pikermian "large" mammal assemblage is characterized by dominance of the families Felidae, Hyaenidae, Equidae, Rhinocerotidae, Bovidae, Giraffidae, and Gomphotheriidae. A great diversity of these horses, rhinoceroses, antelopes, giraffes, and distant relatives of elephants, and a poor representation of the deer (family Cervidae) is typical for this paleobiome (1–3, 7–8). The Pikermian paleobiome had a vast geographic range. Its core area was the SubParatethyan region that extended from the Balkans in the west to Afghanistan in the east, but it ranged much further and included multiple large mammal carnivore and ungulate lineages in common with East Asia and Africa.

Despite this broad agreement regarding the timing and environmental setting of the Pikermian paleobiome, little is known about the details of its distribution in space and time, apart from a study of the northeastern Mediterranean area showing the effect of regional differences in habitat on the occurrence of closed-habitat taxa, especially primates and medium-sized carnivores (9, 10). In a general sense the development of the Pikermian paleobiome is related to the phenomenon of mid-latitude drying, connected to the uplift of Tibetan Plateau and the redistribution of precipitation in Northern Hemisphere following the uplift (11, 12). Climate model runs (e.g., 11–15) suggest that the uplift of the Tibetan Plateau alone would be enough to establish considerable drying of Central Asia and monsoon circulation in East Asia. The modeled results closely resemble the environmental changes that are observed around 7–8 Ma in South and East Asia (e.g., 5, 16–22).

In the Eastern Mediterranean, there was high seasonality in the Late Miocene (Tortonian Stage), and there was increasing summer drought from the Tortonian to the Messinian Stages (latest Miocene) (23). During the Messinian there was high evaporation and low rainfall in the eastern Mediterranean, with lower seasonality because of increased duration of summer aridity (24). There is less evidence about the detailed effects of mid-latitude drying on western Asia. Here we use the history of changing geographic extent of the Pikermian chronofauna to investigate the regional evolution of the mid-latitude drying in western Asia, and the additional regional factors determining the details of its spatial and temporal extent. The characteristic Pikermian mammal assemblage may be considered a chronofauna in the sense of Olson (25). The purpose of the present study is to chart its development in space and time and to relate its history to climatic and environmental changes. We use occurrence data for fossil mammal data from the NOW database (26) and Faunal Resemblance Index for the genus taxonomic rank (GFRI) to map the extent of the Pikermian chronofauna, using the genus listing for Pikermi as the standard of comparison. We use the hypsodonty proxy (5, 27, 28) to map paleoprecipitation distributions and the humidity setting of individual fossil localities. To present our mammal data in a larger context, we use a climate model experiment for the Late Miocene with a fully coupled atmosphere-ocean general circulation model.

Results

The Pikermian faunal record represents the climate history of the Late Miocene. Similar to (23), we use the climate modeling to set the mammal proxy data into a larger-scale climatic context. The Tortonian model run illustrates higher rainfall (Fig. 1*A*) for

Author contributions: J.T.E., M.M.A., R.L.B., and M.F. designed research; J.T.E., M.M.A., A.M., and M.F. performed research; J.T.E., M.M.A., and A.K. contributed new reagents/analytic tools; J.T.E., M.M.A., A.M., A.K., and M.F. analyzed data; and J.T.E., M.M.A., A.M., R.L.B., and M.F. wrote the paper.

The authors declare no conflict of interest.

This article is a PNAS Direct Submission.

[1]To whom correspondence should be addressed. E-mail: jussi.t.eronen@helsinki.fi.

This article contains supporting information online at www.pnas.org/cgi/content/full/0902598106/DCSupplemental.

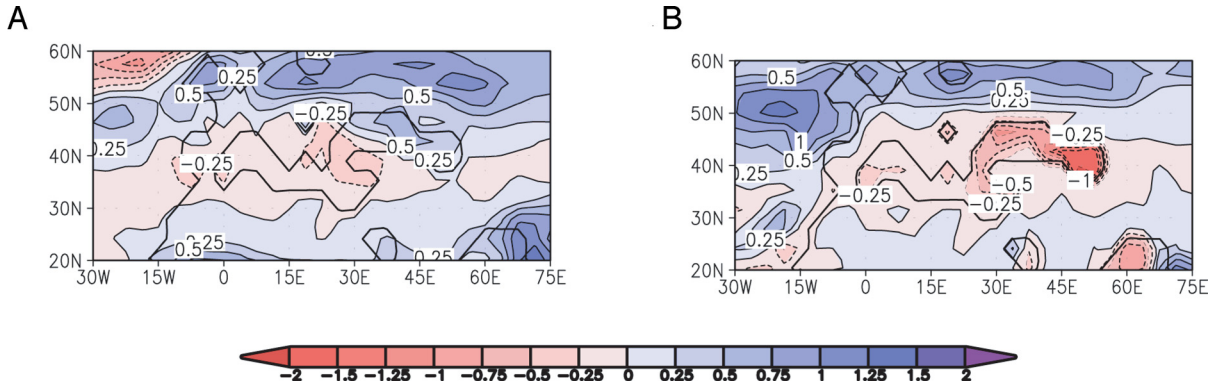

Fig. 1. The annual average anomalies for (*A*) precipitation (in mm/d), and (*B*) precipitation minus evaporation (mm/d) of the Late Miocene experiment as compared to the present-day control run.

Central to Eastern Europe, whereas the Mediterranean realm shows less precipitation than the present-day control experiment. Patterns of precipitation minus evaporation (Fig. 1*B*) are quite comparable to precipitation differences between the Tortonian and the control run. However, P-E demonstrate the pronounced increase in aridity in the Eastern Mediterranean and Paratethys region. In the following, we will show that the decrease of precipitation around the eastern Mediterranean in the Tortonian simulation corresponds closely to the extent of the Pikermian paleobiome during this time (Fig. 2).

We investigated an interval spanning the latest Middle Miocene to the medial Pliocene, (12–3.4 Ma) divided into 8 timeslices centered on the European Neogene fossil mammal (MN) biochronologic units MN7 + 8, MN9, MN10, MN11, MN12, MN13, MN14, and MN15 [Fig. 2, see also Fig. S1 for full-sized images] (see 29–32 for the definition of MN system). In the absence of any prior quantification we arbitrarily include local faunal lists in the Pikermian chronofauna if the locality has GFRI value equal to or higher than 0.7.

At the end of the Middle Miocene during MN7 + 8 (13.5–11.1 Ma ago, Fig. 2 *B* and *C*, level I), genus similarity to Pikermi was still low. By our criterion, the only occurrence of a Middle Miocene Pikermian chronofauna site in this dataset is (barely) the locality Yeni Eskisahar 1 in Anatolia (Raup–Crick GFRI 0.695). There are no localities of this age in Central Asia, and the coloring in this area is only suggestive, based on interpolation from the next younger timeslice (MN9).

By the beginning of the Late Miocene, in the time slice centred on MN9 (11.1–9.7 Ma ago, Fig. 2 *B* and *C*, II), there were already several localities representing the Pikermian chronofauna in the Eastern Mediterranean-West Asian region: Eldari I in Georgia, Esme Akcaköy, Akin and Middle Sinap in Turkey, and Pentalophos 1 in Greece. In Central Europe Vösendorf, Austria also has a high GRFI value.

From the MN 9/10 transition onward (9.7–8.7 Ma ago, Fig. 2 *B* and *C*, III), the Pikermian similarity area increases rapidly. Among localities with high similarity outside the core region are Udabno I in Georgia and Sant Miguel de Taudell in Spain. By MN11 (8.7–8.0 Ma ago, Fig. 2 *B* and *C*, IV) the area is already close to its maximum extent, with the westernmost occurrences of high similarity at Puente Minero in Spain and Dorn Dürkheim 1 in Germany.

The Pikermian chronofauna had its acme in the time slice centred on MN12 (8.0–6.6. Ma ago, Fig. 2 *B* and *C*, V), when it was distributed widely throughout Europe and Central Asia, including the classic Pikermian localities of Maragheh, Samos, and Pikermi (6). The GFRI is generally very high in the Eastern Mediterranean area [e.g., Kavakdere (Sinap 26) and Çobanpınar (Sinap 42) in Anatolia, and Samos in Greece], extending also to Iran (Maragheh), the Balkans, the Pannonian Basin (Hungary),

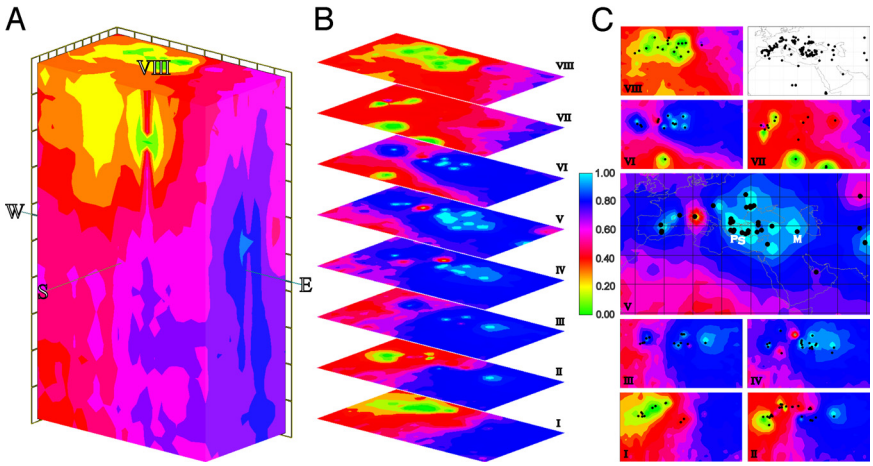

Fig. 2. Raup–Crick genus-level faunal similarity to Pikermi, using inverse temperature colors to avoid confusion with the hypsodonty map (Fig. 3). High similarity is indicated by blue colors, low similarity by reds, yellows, and greens. Dots indicate the positions of localities of the interval in question. (*A*) Spatiotemporal block generated in RockWorks. (*B*) Stacked and inclined timeslice images to show temporal change in distribution patterns. (*C*) Face-on view of timeslices, MN12 (V) enlarged and present-day base map with all localities shown. I, MN7 + 8; II, MN9; III, MN10; IV, MN11; V, MN12; VI, MN13; VII, MN14; VIII, MN15; P, Pikermi; S, Samos; M, Maragheh.

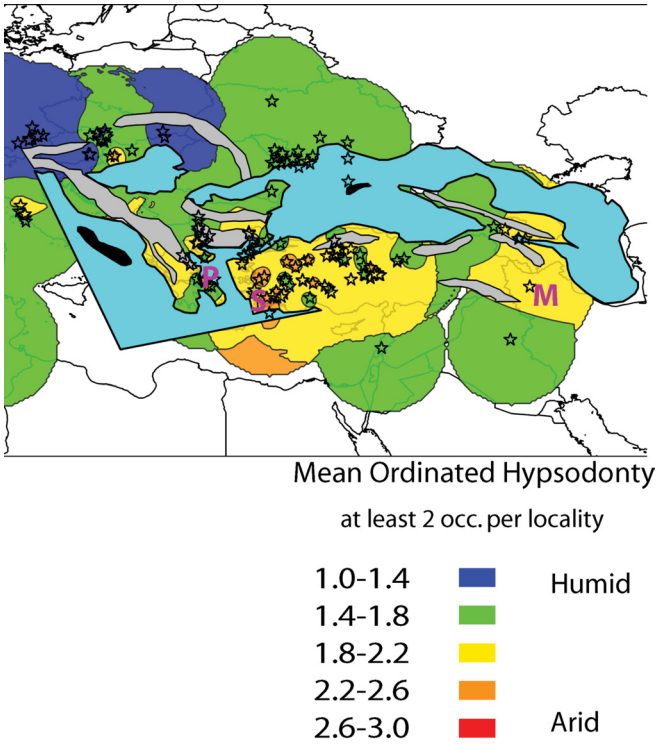

Fig. 3. Map of tooth crown height for the Late Miocene of the Eastern Mediterranean and surrounding areas. We use a map based on (51) to schematically represent the paleogeography of Late Miocene situation. Water is indicated by light blue, mountains by gray. Asterisks show the localities used for interpolating the color patterns. P, Pikermi; S, Samos; M, Maragheh. See text for other explanations.

and the Northern coast of the Black Sea. The data from the Iberian Peninsula also show similar pattern with high similarity to Pikermi.

In the Late Miocene time slice, MN13 (6.6–5.3 Ma ago, Fig. 2 *B* and *C*, VI), the pattern begins to change. While Greece, Anatolia and Caucasus/Iran remains an area with high similarity index values, Central Europe and especially the Iberian Peninsula now display much lower similarity to Pikermi. The data from Central Asia and East Africa (not shown) show only medium similarity values. The Early Pliocene, MN14 and MN15 (5.3–3.4 Ma, Fig. 2 *B* and *C*, VII–VIII), is relatively poorly sampled but available data suggest that the Pikermian chronofauna has now vanished, even from Anatolia.

We used mean ordinated tooth crown height or hypsodonty (5, 33–34) to map the humidity context of the Pikermian biome (Fig. 3). The Late Miocene hypsodonty pattern reveals the emergence of more arid-adapted and hence more hypsodont (5, 28) faunas, dominated by bovids and horses, in the Eastern Mediterranean region and Central Asia (see 2, 27, 28 for more thorough analysis of this pattern). The persistently more humid areas of low hypsodonty are in Western Europe and in Eastern Europe north of the Paratethys, outside the geographic range of the Pikermian chronofauna. Although there is no straightforward correlation between mean hypsodonty and Pikermian GFRI ($R^2 = 0.135$), comparing the combined GFRI values for the interval 7–11 Ma (Fig. 4) reveals a close resemblance between the hypsodonty pattern and the similarity pattern for the Late Miocene time slices, supporting the conventional view of a close relationship between open environments and the Pikermian chronofauna. The low statistical correlation between hypsodonty and GRFI values is partly explained by the fact that many localities with high GFRI have many carnivores, which are not included in the hypsodonty proxy.

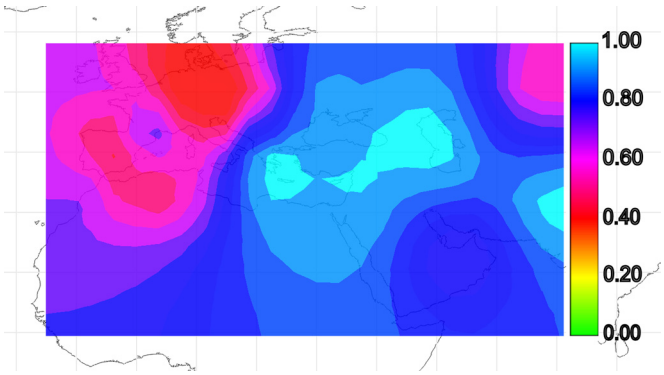

Fig. 4. Cumulative map of the Raup–Crick–similarity index values as compared to the locality of Pikermi for the interval 11 to 7 Ma, which corresponds to the Late Miocene experiment model run.

Discussion

The rise and fall of the Pikermian chronofauna corresponds to the expansion and contraction of seasonal aridity regimes in the Eastern Mediterranean from the Middle Miocene to the Early Pliocene. Results of a Tortonian model simulation suggests that this region is influenced by several processes that resulted in the adaptive radiation and geographic extension of the Pikermian chronofauna. These processes are related to the Central American Isthmus, the absence of the Greenland ice sheet and Greenland's lower elevation, palaeogeographic changes in Eurasia, and environmental changes in North Africa. Ocean heat transport is a major factor influencing Cenozoic climate evolution (35). When the Central American Isthmus was open, there was a weakened northward heat transport in the Atlantic Ocean (e.g., 36, 37). Our Tortonian simulation indicates that the atmosphere compensated for the reduced ocean heat transport, and Fig. 1 illustrates the increased atmospheric moisture transport into the European realm. The subsequent closure of the Panama Strait affected climate evolution in Europe. Other palaeogeographic changes also influenced the Cenozoic climate evolution (e.g., 11, 38). The Greenland ice-sheet has been removed in our Tortonian simulation and lower elevation also led to modifications of atmospheric circulation (Fig. S2, *cf.* 39), in that Europe received increased moisture transport from the North Atlantic. Other climate model results suggest that the Eastern Mediterranean region became more arid from "the Miocene" to the present, because of the uplift of the Tibetan Plateau and the shrinkage of the Paratethys Sea (40). Finally, the climate in Europe was also influenced by vegetation changes in North Africa around the Miocene/Pliocene boundary (41). A detailed explanation of how the relevant processes affected the climate in the Late Miocene would go beyond the scope of the present study. In the following we discuss how the changes we observe in the geographic extent of the Pikermian chronofauna relate to previously proposed scenarios of environmental change and to our climate model results.

The impact of the Late Miocene climate change on the land biota was considerable. The most marked was probably the Mid-Vallesian Crisis (9.6 Ma ago) (42, 43) that resulted in extinction of many faunal lineages in western Europe, especially taxa associated with closed habitats (4), including hominoid primates. It has been suggested that the reason for Mid-Vallesian Crisis was change in the vegetation structure from tropical evergreen to deciduous forest and woodland. It has been proposed (43) that this shift was caused by altered oceanic and atmospheric circulation patterns. This hypothesis is supported by our results.

The maximum extent of the Pikermian chronofauna occurred in MN 12, Late Tortonian Stage, approximately 7.5 Ma ago (44, 10).

There is emerging evidence that large mammalian lineages also extended into Africa during the Late Miocene (45). The first contraction in the geographic extent of the Pikermian chronofauna is already visible during latest Miocene, MN13 (6.6–5.3 Ma), when the hypsodonty maps (see 5, 27, 28) suggest that the Mediterranean realm was at its driest. By our faunal similarity criteria, the Pikermian chronofauna became extinct in Western Eurasia by the Early Pliocene, approximately 5 Ma ago. By this time, the predominantly east-west oriented, humidity-driven hypsodonty pattern in Europe was also replaced by a north-south oriented pattern, presumably driven primarily by temperature (5).

During the Early Pliocene precipitation decreased in Central Europe (46), but the Eastern Mediterranean region was a refugium for Central European flora (47), with humid conditions. While the paleofloral interpretation of the Eastern Mediterranean Early Pliocene is somewhat inconclusive (47, 48), its spotty floral record shows open-woodlands, broad-leaf evergreen taxa and humid sclerophyllous taxa (49). A more humid Mediterranean with a drier Central Europe suggests a shift to a circulation pattern with decreased westerlies toward Central Europe and increased westerlies in the Mediterranean region. Based on these data, it seems that there was increased regional differentiation of habitats during the early Pliocene.

The climatic and environmental changes of the latest Miocene were detrimental to the large land mammals, and a possible explanation for the extinction of the Pikermian chronofauna in its core area could be the "double whammy" of increased seasonality and regional differentiation, followed by significantly increased humidity and forestation. Such an explanation would explain that it was the large, wide-ranging, open-adapted taxa that were severely affected, while small mammals were hardly affected at all (32). Even though the hypsodonty map (5) shows that dry conditions continued in Anatolia in the Pliocene, the Pikermian chronofauna was gone.

Materials and Methods

We downloaded the dataset used from the NOW database on July 4th, 2007 (26). We used all large mammal data which was between 11 and 4 Ma in age. This encompasses European Neogene Mammal units MN7 to MN15. We calculated different genus faunal resemblance indexes (GFRI) to the locality of Pikermi from the dataset using the PAST (50, see http://folk.uio.no/ohammer/past/). We used Jaccard, Dice, and Raup–Crick GFRIs to compare differences in the overall trends and between different GFRIs. We show results only for Raup–Crick GFRI (also see Table S1). The other GFRIs give similar results.

We applied the following criteria for undertaking these analyses: taxonomic identification at least to the genus level; at least 7 taxa identified for each locality; geographic coordinates for the locality available. We tested our method with different minimum numbers of taxa. We found that when we used less than 7 taxa the analytical noise increased, and when we limited our analysis to localities with 10 or more taxa, the number of available localities was very low. Overall, we found the number of taxa used did not affect the spatial geographic patterns: the east-west and north-south dispersion of localities was essentially the same and the pattern was robust.

The results from GFRIs were imported to RockWorks 2002 where we extrapolated the point data to a grid that covers the whole area under investigation. This was done using solid model function in Rockworks. This produced a 3-dimensional block covering the study area. From the block we took slices, using plan function, at Z levels corresponding to each MN unit. These were plotted on the top of the present-day world map.

We used herbivore molar tooth crown height as a rough proxy for humidity (see 5, 27, 28). All small mammals (orders Lagomorpha, Chiroptera, Rodentia, and Insectivora) as well as carnivores (orders Carnivora and Creodonta) were deleted. After this, all singletons, sites containing only 1 taxon occurrence, were deleted. We plotted the data using MapInfo 8.5 and Vertical Mapper 3.0, using the following initial settings: Cell size 20 km, Search radius 500 km, Grid border 500 km, 10 inflections, values rounded to nearest 0,1. The interpolated maps were then imported as grids to Vertical Mapper, where they were assigned to 5 classes and then contoured to connect the areas with similar values. See Table S2 for localities used. We used the Late Miocene map from Popov et al. (51), overlayed to present-day map to show the paleogeographic setting.

We compared the mean hypsodonty values and the Pikermi GFRI values with standard statistics using JMP 7.01 for Macintosh. Comparisons were made with those localities for which we could calculate both values. See (Table S1).

To investigate the climate processes involved in the demise of mammalian chronofauna, we used results from the fully-coupled atmosphere-ocean general circulation model (AOGCM) ECHAM5/MPIOM. The setup for model runs were as follows: the resolution used was T31L19 (3.75°) for the atmosphere and GR30L40 (≈3°) for the ocean. We also consider a proxy-based reconstruction for the palaeovegetation (see 52). The boundary conditions (e.g., the paleorography, paleovegetation) refer to the Late Miocene, and are based on previous (e.g., 39, 52) model runs.

The palaeorography (Fig. S3) was generally lower than today. For example, the height of the Tibetan Plateau is about 70% of its recent elevation, and Greenland is also much lower because of the absence of the present-day ice-sheet. Due to the coarse model resolution, the palaeogeography is largely equal to the modern land-sea distribution, but it includes the Paratethys (see Fig. S3) and particularly the ocean model includes an open Central American Isthmus. For the present-day control run and the Tortonian run, atmospheric CO_2 is specified with 360 ppm. We integrated the model over 2,500 years to bring it into its dynamic equilibrium. For the data analysis, we take monthly averages of the last 10 simulation years.

ACKNOWLEDGMENTS. We thank Juha Lento (Scientific Computing, Ltd.) for technical assistance in performing the climate model runs and John Kutzbach for patient guidence and many good suggestions during the development of this paper. This work was supported by The Academy of Finland (M.F.); Helsingin Sanomain 100-vuotissäätiö and Kone Foundation (J.T.E.), Deutsche Forschungsgemeinschaft Project FOR-1070 (to A.M.), the federal state Hessen (Germany) within the LOEWE initiative (A.M.), and National Science Foundation Grants 0125009 (to R.L.B.) and BCS-0321893 (to F. Clark Howell and Tim White). CSC–Scientific Computing Ltd. (Finland) supercomputers were used for climate computations.

1. Bernor RL, Andrews PA, Solounias N, van Couvering JA (1979) The evolution of ''Pontian'' mammal faunas: some zoogeographic, palaeoecological, and chronostratigraphic considerations. *The VIIth Inter Congr Medit Neogene Annales Pays Helleneniques, h ser* 1:81–89.
2. Bernor RL (1983) in *New Interpretations of Ape and Human Ancestry*, eds Ciochon RL, Corruccini RS (Plenum Press, New York), pp 21–64.
3. Bernor RL (1984) A zoogeographic theater and a biochronologic play: The time/biofacies phenomena of Eurasian and African Miocene mammal provinces. *Paléobiologie Continentale* 14:121–142.
4. Fortelius M, et al. (1996) in *The Evolution of Western Eurasian Neogene Mammal Faunas*, eds Bernor RL, Fahlbusch V, Mittmann H-V (Columbia Univ Press, New York). pp 414–448.
5. Fortelius M, et al. (2002) Fossil mammals resolve regional patterns of Eurasian climate change during 20 million years. *Evol Ecol Res* 4:1005–1016.
6. Bernor RL, Solounias N, Swisher CC III, Van Couvering JA (1996) in *The Evolution of Western Eurasian Neogene Mammal Faunas*, eds Bernor RL, Fahlbusch V, Mittmann H-V (Columbia Univ Press, New York), pp 137–15.
7. Solounias N, Plavcan JM, Quade J, Witmer L (1999) in *The evolution of Neogene terrestrial ecosystems in Europe*, eds Agustí J, Rook L, Andrews P (Cambridge Univ Press, Cambridge), pp 436–453.
8. Agustí J, Anton M (2002) in *Mammoths, Sabertooths and Hominids. 65 Million Years of Mammalian Evolution in Europe* (Columbia Univ Press, New York), p 313.
9. Koufos GD (2006) Palaeoecology and chronology of the Vallesian (late Miocene) in the Eastern Mediterranean region. *Palaeogeogr Palaeoclimatol Palaeoecol* 234:127–145.
10. Kostopoulos DS (2009) The Pikermian Event: Temporal and spatial resolution of the Turolian large mammal fauna in SE Europe. *Palaeogeogr Palaeoclimatol Palaeoecol* 274:82–95.
11. Kutzbach JE, Prell L, Ruddiman WF (1993) Sensitivity of Eurasian climate to surface uplift of the Tibetan Plateau. *J Geol* 101:177–190.
12. Broccoli AJ, Manabe S (1997) in *Tectonic Uplift and Climate Change*, ed Ruddiman WF (Plenum Press, New York), pp 89–121.
13. Ruddiman WF, Kutzbach JE (1989) Forcing of late Cenozoic Northern Hemisphere climate by plateau uplift in Southern Asia and American West. *J Geophys Res* 94:18409–18427.
14. Ruddiman WF, Kutzbach JE (1990) Late Cenzoic plateau uplift and climate change. *Trans R Soc Edinb Earth Sci* 81:301–314.
15. Liu X, Yin Z-Y (2002) Sensitivity of East Asian monsoon climate to the uplift of the Tibetan Plateau. *Palaeogeogr Palaeoclimatol Palaeoecol* 183:223–245.
16. Sun D, Shaw J, An Z, Cheng M, Yue L (1998) Magnetostratigraphy and paleoclimatic interpretation of a continous 7.2. Ma Late Cenozoic eolian sediments from the Chinese Loess Plateau. *Geophys Res Lett* 25:85–88.
17. Ding ZL, et al. (1999) Pedostratigraphy and paleomagnetism of a ≈7 Ma eolian loess-red clay sequence at Lingtai, Loess Plateau, north-central China and the implications for paleomonsoon evolution. *Palaeogeogr Palaeoclimatol Palaeoecol* 152:49–66.

18. Qiang XK, Li ZX, Powell, C McA, Zheng HB (2001) Magnetostratigraphic record of the Late Miocene onset of the East Asian monsoon, and Pliocene uplift of northern Tibet. *Earth Planet Sci Lett* 187:83–93.
19. Quade J, Cerling TE (1995) Expansion of C4 grasses in the Late Miocene of northern Pakistan: evidence from stable isotopes of paleosols. *Palaeogeogr Palaeoclimatol Palaeoecol* 115:91–116.
20. Quade J, Cerling TE, Bowman JR (1989) Development of Asian monsoon revealed by marked ecological shift during the latest Miocene in Northern Pakistan. *Nature* 342:163–166.
21. Kroon D, Steens T, Troelstra SR (1991) in *Proceedings of the Ocean Drilling Project Scientific Results*, eds Prell WL, et al. (Ocean Drilling Program, College Station, TX), pp 257–263.
22. Hoorn C, Ohja T, Quade J (2000) Palynological evidence for vegetation development and climatic change in the sub-Himalayan zone (Neogene, Central Nepal), *Palaeogeogr Palaeoclimatol Palaeoecol* 163:133–161.
23. Brachert TC, et al. (2006) Porites corals from Crete (Greece) open a window into Late Miocene (10 Ma) seasonal and interannual climate variability. *Earth Planet Sci Lett* 245:81–94.
24. Mertz-Kraus R, Brachert TC, Reuter M (2008) *Tarbellastraea* (Scleractinia): A new stable isotope archive for Late Miocene paloenvironments in the Mediterranean. *Palaeogeogr Palaeoclimatol Palaeoecol* 257:294–307.
25. Olson EC (1952) The evolution of Permian Vertebrate Chronofauna. *Evolution* 6:181–196.
26. Fortelius, M (2007) Neogene of the Old World Database of Fossil Mammals (NOW). University of Helsinki. http://www.helsinki.fi/science/now/.
27. Fortelius M, et al. (2006) Late Miocene and Pliocene large land mammals and climatic changes in Eurasia. *Palaeogeogr Palaeoclimatol Palaeoecol* 238:219–227.
28. Eronen JT (2006) Eurasian Neogene large herbivorous mammals and climate. *Acta Zoologica Fennica* 216:1–72.
29. Mein P (1975) in *Report on Activity of the RCMNS Working Group (1971-1975)*, ed Senes J (Regional Committee on Mediterranean Neogene Stratigraphy (RCMNS), Bratislava), pp 78–81.
30. Mein P (1989) In *European Neogene Mammal Chronology. NATO ASI series* Vol. 180, eds Lindsay EH, Fahlbusch V, Mein P (Plenum Press, New York), pp 73–90.
31. Bruijn de H, et al. (1992) Report of the RCMNS working group on fossil mammals, Reisensburg 1990. *Newsl Stratigr* 26:65–118.
32. Agustí J, et al. (2001) A calibrated mammal scale for the Neogene of Western Europe. State of the art. *Earth-Science Rev* 52:247–260.
33. Damuth J, Fortelius M (2001) in *EEDEN Plenary Workshop on Late Miocene to early Pliocene Environments and Ecosystems*, eds Agustí J, Oms O (EEDEN Programme, European Science Foundation, Sabadell, Spain), pp 23–24.
34. Janis C, Fortelius M (1988) On the means whereby mammals achieve increased functional durability of their dentitions, with special reference to limiting factors. *Biol Rev (Cambridge)* 63:197–230.
35. Bice KL, Scotese CR, Seidov D, Barron EJ, (2000) Quantifying the role of geographic change in Cenozoic ocean heat transport using uncoupled atmosphere and ocean models. *Palaeogeogr Palaeoclimatol Palaeoecol* 161:295–310.
36. Mikolajewicz U, Crowley T J, (1997) Response of a coupled ocean/energy balance model to restricted flow through the central American isthmus. *Palaeoceanography* 12:429–441.
37. Mikolajewicz U, Maier-Reimer E, Crowley TJ, Kim KJ, (1993) Effect of Drake and Panamanian gateways on the circulation of an ocean model. *Palaeoceanography* 8:409–426.
38. Ruddiman WF, Kutzbach JE, Prentice IC, (1997) in *Tectonic Uplift and Climate Change*, ed Ruddiman WF (Plenum Press, New York), pp 203–235.
39. Steppuhn A, Micheels A, Geiger G, Mosbrugger V (2006) Reconstructing the Late Miocene climate and oceanic heat flux using the AGCM ECHAM4 coupled to a mixed-layer ocean model with adjusted flux correction. *Palaeogeogr Palaeoclimatol Palaeoecol* 238:399–423.
40. Fluteau F, Ramstein G, Besse J (1999) Simulating the evolution of the Asian and African monsoons during the past 30 Myr using an atmospheric general circulation model. *J Geophys Res* 104:11995–12018.
41. Micheels A, Eronen J, Mosbrugger V (2009) The Late Miocene climate response to a modern Sahara desert. *Glob Planet Change* 67:193–204.
42. Agusti J, Moya-Sola S (1990) Mammal extinctions in the Vallesian (Upper Miocene). *Lecture Notes in Earth Science* 30:425–432.
43. Agusti J, Sanz de Siria A, Garces M (2003) Explaining the end of the hominoid experiment in Europe. *J Hum Evol* 45:145–153.
44. Kostopoulos DS, Sen S, Koufos GD (2003) Magnetostratigraphy and revised chronology of the Late Miocene mammal localities of Samos, Greece. *Intl J Earth Sci* 92:779–794.
45. Bernor RL, Rook L, Haile Selassie Y (in press) *Biogeography Ardipithecus kadabba: Late Miocene Evidence from the Middle Awash, Ethiopia*, (University of California Press).
46. Mosbrugger V, Utescher T, Dilcher D (2005) Cenozoic continental climatic evolution of Central Europe. *Proc Natl Acad Sci USA* 102:14964–14969.
47. Kovar-Eder J (2003) in *Distribution and Migration of Tertiary Mammals in Eurasia. A volume in honour of Hans de Bruijn*, eds Reumer JWF, Wessels W (Deinsea 10, Utrecht, The Netherlands),pp 373–392.
48. Kloosterboer-van Hoeve M (2000) Cyclic changes in the late Neogene vegetation of northern Greece. *LPP Contributions Series* 11:1–131.
49. Kovar-Eder J, Jechorek H, Kvacek Z, Parashiv V (2008) The integrated plant record: An essential tool for reconstructing Neogene zonal vegetation in Europe. *Palaios* 23:97–111.
50. Hammer, Ø, Harper, DAT, Ryan, PD (2001) PAST: Paleontological statistics software package for education and data analysis. *Palaeontologia Electronica* 4: http://palaeo-electronica.org/2001_1/past/issue1_01.htm.
51. Popov SV, et al. (2004) Lithological-Paleogeographic maps of the Paratethys. *Courier Forschung-Institut Senckenberg* 250:1–46.
52. Micheels A, Bruch AA, Uhl D, Utescher T, Mosbrugger V (2007) A late Miocene climate model simulation with Echam4/ML and its quantitative validation with terrestrial proxy data. *Palaeogeogr Palaeoclimatol Palaeoecol* 253:267–286.